České vysoké učení technické v Praze, Fakulta stavební

Czech Technical University in Prague, Faculty of Civil Engineering

Doc. Ing. Pavel Novák, PhD.

Současný pokrok při modelování globálního tíhového pole

Recent advances in global gravity field modeling

Souhrn

Geodézie se tradičně snaží o měření a popis zemského tíhového pole. Přesná a spolehlivá znalost tíhového pole slouží pro správnou interpretaci a redukci různých geodetických měření prováděných pod vlivem zemské tíže. Povrchová tíhová data představovala po dlouhou dobu jediný dostupný zdroj informace o zemském tíhovém poli. Návrhy na nové měřické postupy a technologie se začaly rychle objevovat po vypuštění první umělé družice Země v roce 1957. Sledování dráhových poruch jednotlivých družic poskytovala nová data, která byla možno použít pro odvození prvních globálních modelů zemského tíhového pole. S nástupem přesné družicové navigace se později začala používat metoda letecké gravimetrie jako doplněk k pozemským datům a globálním modelům.

Významný pokrok při globálním mapování zemského tíhového pole je v současnosti dosahován s pomocí nových družicových misí určených pro výzkum tíhového pole. První z celkem tří v současnosti plánovaných a částečně již realizovanvých družic tohoto typu byla vypuštěna v roce 2000. Další byla vypuštěna v roce 2002 a poslední bude vyslána na oběžnou dráhu v roce 2007. Tyto projekty jsou předeším určeny pro sběr dat různého druhu a vlastností, která mohou být použita pro odvození statického a časově proměnného tíhového pole s dříve nedostupnou přesností a prostorovým rozlišením. Tyto produkty budou sloužit nejen samotné geodézii, ale umožní mezioborový výzkum v řadě geověd včetně fyziky pevné Země a oceánografie.

Protože tyto mise nyní představují páteř výzkumných aktivit v oblasti geodézie, tento text představuje jejich stručný souhrn. V úvodu textu jsou velmi krátce představeny teoretické základy teorie potenciálu včetně v tomto textu použitých parametrů, symbolů a fyzikálních zákonů. Neznámé parametry popisující zemské tíhové pole jsou vztaženy k dostupným družicovým datům poskytovanými jednotlivými misemi. Geodézie řeší vedle skalárního popisu zemského tíhového pole také jeho geometrickou reprezentaci ve smyslu hladinové plochy, která reprezentuje střední nerušenou hladinu světových oceánů – geoid. Jeho řešení je také velmi stručně nastíněno.

Jednotlivé principy družicových měření jsou prezentovány v tomto textu na pozadí teoretického základu včetně jejich konkrétních realizací v podobě stávajících družicových misí. Hlavní výhody a očekávaný přínos každé mise jsou vysvětleny z pohledu poskytovaných dat. Inverze jednoho vybraného typu dat je nastíněna v podobě zjednodušeného matematického modelu. Ten slouží jako příklad pro zpracování obecného typu dat z dalších družicových misí určených pro výzkum tíhového pole. Stávající a navrhované aplikace pro nové přesné modely tíhového pole jsou načrtnuty ve smyslu tří hlavních aplikačních oblastí: geodézie, fyziky pevné Země a oceánografie. Dostupné parametry současných modelů jsou v závěru textu porovnány s požadavky na přesnost a prostorové rozlišení vybraných konkrétních aplikací.

Summary

Traditionally geodesy has been attempting to measure and describe the Earth's gravity field. Its precise and reliable knowledge serves for correct interpretation and reduction of various geodetic observations collected in the presence and under the influence of Earth's gravity. For a long time ground gravity data had been the only available information on the Earth's gravity field. With the launch of the first artificial satellite in 1957, new observation techniques were quickly proposed. Measured orbital perturbations of various satellites started to deliver new types of data useful for derivation of first global gravity field models. Later, with the advent of precise satellite-based positioning, airborne gravity observations became complementary to ground gravity and global gravity models.

Most recently, significant advances in global gravity field mapping have been achieved through deployment of gravity-dedicated satellite missions. The first satellite from three currently planned and partly realized missions was launched in 2000. The second satellite mission was launched in 2002 and the last satellite should be put to the orbit in 2007. These projects are primarily designed for gathering satellite tracking data of different types and properties that can be used for derivation of static and time-varying gravity fields with unprecedented accuracy and spatial resolution. These products will serve not only to geodesy itself but they will allow for multi-disciplinary research including other geosciences such as the solid Earth physics and oceanography.

As these missions represent a backbone of current research activities in geodesy, this text intends to summarize briefly these efforts. Theoretical foundations of the potential theory are briefly reviewed in the beginning introducing used parameters, notations, and basic physical laws used in geodesy. Unknown parameters describing the Earth's gravity field are related to available satellite tracking data as provided by satellite missions. Besides solving for scalar description of the vector gravity field, geodesy is particularly keen on solving geometric representation of the gravity field in terms of an equipotential surface approximating a mean undisturbed sea level – the geoid. Its solution is also briefly outlined in the text.

On the background of theoretical foundations, satellite observation techniques are presented and their realization in the frame of existing satellite missions is reviewed. Main advantages and anticipated contribution of each particular mission are explained in view of provided data. Inversion of one data type is outlined using a simplified mathematical model. It serves as an example for processing of general spaceborne data from the gravity-dedicated satellite missions. Currently available products are introduced and compared to global gravity models based on traditional observation techniques. Existing and proposed applications for the new precise gravity field models are outlined in terms of three major application areas: geodesy, solid Earth physics and oceanography. Achieved accuracy of recent gravity solutions is compared against accuracy and resolution requirements of selected applications.

Klíčová slova : geodézie · zemské tíhové pole · gravitační zrychlení a potenciál · geoid · družicová mise pro výzkum zemského tíhového pole · gravimetrie · gradiometrie · sférická harmonická řada · Greenova integrace · fyzika pevné Země · oceánografie

Key words : geodesy · Earth's gravity field · gravitational acceleration and potential · geoid · gravity-dedicated satellite mission · gravimetry · gradiometry · spherical harmonic series · Green's integration · solid Earth physics · oceanography

---

České vysoké učení technické v Praze, Fakulta stavební

Název: Současný pokrok při modelování zemského tíhového pole

Autor: Doc. Ing. Pavel Novák, PhD.

Počet stran: 30

Náklad: 150 výtisků

ISBN

Contents

1 Introduction

Gravitation. *The universal force of attraction acting between all matter. It is by far the weakest known force in nature and thus plays no role in determining the internal properties of everyday matter. Due to its long reach and universality, however, gravitation shapes the structure and evolution of stars, galaxies, and the entire universe.*
(Encyclopædia Britannica © 1999 – 2000)

The branch of geosciences dealing with obtaining precise measurements of the Earth, describing its geometry and motion, and mapping its gravity field is known as geodesy. While parameters describing the geometry and rotation of the Earth are known with a relatively high level of accuracy, current knowledge of its gravity field is incomplete and relatively inaccurate. Up to now, data from several dozen satellites had to be combined to produce a single global model of the Earth's gravity field. Such a model does a good job at describing large-scale features of the gravity field but cannot resolve small spatial fluctuations and temporal variations due to mass distribution shifts inside the solid Earth, oceans and atmosphere.

Substantial improvement of our knowledge of the Earth's gravity field is coming by exploiting new approaches based on spaceborne gravity observations. First attempts to design artificial satellites dedicated to mapping the Earth's gravity field date back to late 1960's. During the last half of a century three different concepts for collecting gravity-related data using low orbiting satellites were proposed. The new era of global gravity field mapping then started in 2000 when a first gravity-dedicated satellite was launched. In 2002, a second satellite based on a different observation principle was put to the orbit. The initial phase of new spaceborne techniques will be completed in 2007 when the first spaceborne gradiometer should be launched.

New satellite missions provide (or will provide) data that are used for derivation of global models of the Earth's gravity field with high spatial resolution (100 km) and to very high accuracy (10^{-5} m s^{-2}). Besides solving for the static field, temporal variations of gravity are also being estimated. These products offer new and fundamental insight into a wide range of multidisciplinary research and application areas including geodesy, physics of the solid Earth, oceanography and hydrology. Recent developments in the research area related to Earth's gravity are briefly described and its most recent results are summarized in this text. The satellite missions dedicated to this task are reviewed including their respective observation principles. To provide an idea about the data and their transformation into unknown parameters, mathematical formulations for data of one of the three satellite missions are provided. Sample results demonstrate significantly improved accuracy and spatial resolution of the new global gravity models based on the gravity-dedicated satellite missions. Their importance and consequences are discussed within the multidisciplinary research fields.

2 Basic principles and observables

The Earth's *gravity field* consists of the gravitational and centrifugal components. Both the centrifugal and gravitational fields are vector fields described uniquely by intensity (acceleration) vectors. The vector of *centrifugal acceleration* acting upon each particle attached to the Earth rotating with the angular velocity vector ω can be computed as follows (Huygens's *Horologium Oscillatorium* 1673)

$$\mathbf{a}(\mathbf{x}) = \omega \times (\ \omega \times \mathbf{x})\ . \tag{1}$$

The symbol $\times$ stands for the vector product. Assuming geocentric Earth-fixed Cartesian coordinates, the 3-D position in Eq. (1) is given by the geocentric radius vector

$$\mathbf{x} \ = \ [\ x \quad y \quad z\ ]^T\ . \tag{2}$$

Throughout this text, all vectors and matrices will be typed in bold. For the known position $\mathbf{x}$ and angular velocity ω, the centrifugal field and its parameters do not represent any problem in the task of describing the Earth's gravity field. Moreover, it applies only to particles attached to the Earth. As such, the centrifugal field will be neglected in the following sections since spaceborne data are only considered.

2.1 Gravitational field of the Earth

The Earth's *gravitational field* as described by Newton's fundamental law of gravitation is also a 3-D vector field (neglecting its temporal variability – thus the fourth dimension). The vector of *gravitational acceleration* (gravitational vector) generated by the Earth of the volume B and mass density distribution ϱ (Newton's *Philosophiae Naturalis Principia Mathematica* 1687) reads

$$\mathbf{g}(\mathbf{x}) \ = \ G \iiint_B \varrho(\mathbf{y})\ \frac{\mathbf{x}-\mathbf{y}}{|\ \mathbf{x}-\mathbf{y}\ |^3}\ \ dB(\mathbf{y})\ , \tag{3}$$

with the universal gravitational constant G, differential volume element dB and the integration point defined by the geocentric radius vector $\mathbf{y}$.

The Earth's gravitational field satisfies (considering some mild approximations) two elementary conditions: it is both conservative and irrotational, i.e.,

$$\oint \mathbf{g}(\mathbf{x}) \cdot d\mathbf{x} \ = 0 \quad \wedge \quad \nabla \times \mathbf{g}(\mathbf{x}) \ = \ \mathbf{o}\ . \tag{4}$$

The symbol $\cdot$ stands for the scalar product, ∇ for the gradient and $\mathbf{o}$ is the null vector, i.e., $|\ \mathbf{o}\ | = \ 0$. As a consequence of Eqs. (4), the gravitational vector field can be described by a scalar function V called the Earth's *gravitational potential.* Its link to the gravitational vector is given as follows:

$$\nabla V(\mathbf{x}) \ = \ -\ \mathbf{g}(\mathbf{x})\ . \tag{5}$$

Applying the gradient operator ∇ one more time, the gravitational potential satisfies the Poisson differential equation, e.g., (Heiskanen and Moritz 1967),

$$\nabla^2 V(\mathbf{x}) \;=\; -\,4\pi G\varrho(\mathbf{x}) \;. \tag{6}$$

The symbol ∇^2 stands for the Laplacian (sometimes the symbol $\triangle$ is used). Moreover, the gravitational potential is also regular at infinity, i.e.,

$$V(\mathbf{x}) \;=\; \mathcal{O}\Big(\,|\,\mathbf{x}\,|^{-1}\Big) \;. \tag{7}$$

In this case, Landau's symbol $\mathcal{O}$ describes linear attenuation of the gravitational potential with an increasing distance from the gravitating masses. Equation (7) also represents a boundary condition: the gravitational potential vanishes at an infinite distance from the gravitating masses; for the Earth, the boundary represents a geocentric sphere with an infinite radius.

The gravitational potential is not directly measurable. Combining Eqs. (3) and (5), it can be represented by the volume integral

$$V(\mathbf{x}) \;=\; G\iiint_B \frac{\varrho(\mathbf{y})}{|\,\mathbf{x}-\mathbf{y}\,|}\;dB(\mathbf{y}) \;. \tag{8}$$

A theoretically simple formula, however, practically not applicable in case of the Earth due to our limited knowledge of its internal mass density distribution ϱ. Fortunately, gravimeters and gradiometers can measure first- and second-order directional derivatives of the gravitational potential, respectively. Thus, gravitational observables are in a form of entries of the gravitational vector (neglecting the centrifugal component), i.e.,

$$\nabla V(\mathbf{x}) \;=\; [\; D_x \quad D_y \quad D_z \;]^T \; V(\mathbf{x}) \;, \tag{9}$$

and/or entries of the *gradiometric tensor*

$$\mathrm{vec}\,[\;\nabla\otimes\nabla V(\mathbf{x})\;] \;=\; \Big[\; D^2_{xx} \quad D^2_{xy} \quad D^2_{xz} \quad D^2_{yy} \quad D^2_{yz} \quad D^2_{zz} \;\Big]^T \; V(\mathbf{x}) \;. \tag{10}$$

The operators D and D^2 stand for the first- and second-order directional derivatives, respectively. The symbol f will be used in this text to symbolize any of these operators including their combinations (such as the Stokes operator, for example). The symbol $\otimes$ in Eq. (10) represents the Kronecker (matrix direct) product, and *vec* is the vectorization command that transforms a matrix into a single column vector. It should be emphasized that not all the entries in Eqs. (9) and (10) must be measurable or measurable with the same level of accuracy. Their availability and accuracy depends on used instrumentation and/or observation technique.

2.2 Parametrization of the gravitational field

The Poisson differential equation given by Eq. (6) for the zero mass density collapses into a homogeneous form

$$\nabla^2 V(\mathbf{x}) \;=\; 0 \;, \tag{11}$$

known as the *Laplace differential equation.* This equation represents foundation for the potential theory that defines and solves various boundary/initial-value problems useful for the solution of the function V with a help of some additional information. In geodesy, this additional information is provided by the observables $f(V)$: entries of the gravitational vector and linearly independent entries of the gradiometric tensor, see Eqs. (9) and (10).

The homogeneous elliptical equation (11) can be solved by separating variables of the gravitational potential. Actually not every coordinate system is suitable for application of this method. The Cartesian coordinate system defined above can be used, however, by far more practical are geocentric *spherical coordinates* defined through the transformations

$$[\, r \quad \theta \quad \lambda \,]^T \; = \; \left[\; \sqrt{x^2+y^2+z^2} \quad \arccos \frac{z}{\sqrt{x^2+y^2+z^2}} \quad \arctan \frac{y}{x} \; \right]^T \; , \tag{12}$$

with the geocentric radius $0 \le r < \infty$, co-latitude $0 \le \theta \le \pi$ and longitude $0 \le \lambda < 2\pi$. In contrary to Cartesian coordinates, their scale coefficients are not equal to one but

$$[\, h_r \quad h_\theta \quad h_\lambda \,]^T \; = [\, 1 \quad r \quad r \, \sin\theta \,]^T \; . \tag{13}$$

The solution of the Laplace differential equation in spherical coordinates has the form of an infinite series, e.g., (Heiskanen and Moritz 1967),

$$\forall \; r \ge R \; : \; V(r,\theta,\lambda) \; = \; \sum_{n=0}^{\infty} \; \sum_{m=-n}^{n} \; \left(\frac{R}{r}\right)^{n+1} \; V_{n,m} \; Y_{n,m}(\theta,\lambda) \; . \tag{14}$$

Stokes's coefficients $V_{n,m}$ of degree n and order m represent **primary unknown values for global gravity field mapping**. Note their physical dimension ($\mathrm{m}^2 \; \mathrm{s}^{-2}$) in Eq. (14). Spherical harmonics $Y_{n,m}$ of degree n and order m read (Abramowitz and Stegun 1972)

$$Y_{n,m}(\theta,\lambda) \; = \; P_{n,m}(\cos\theta) \; e^{im\lambda} \; , \tag{15}$$

with associated Legendre functions of the first kind $P_{n,m}$ (Hobson 1931). Both the Stokes coefficients and spherical harmonics are fully-normalized in numerical applications.

The series in Eq. (14) is uniformly convergent on or outside the so-called Brilloiun sphere (encompassing all gravitating masses) of radius R, i.e., for $r \ge R$. The series form of the gravitational potential nicely describes the per-degree logarithmic attenuation of the gravitational field with an increasing altitude above the Brilloiun sphere: the *attenuation factor* $(R/r)^{n+1}$ also represents the major drawback of spaceborne data – the gravitational field is being smoothed up with the distance from the Earth. The natural method for counteracting this physical property of the gravitational field (differentiation) is discussed later in the text.

The apparatus of the spherical harmonic series is very convenient. However, it has yet another disadvantage: to describe the function V completely, an infinite number of Stokes's coefficients must be known requiring for the series an infinite amount of time to be summed up. In practice, the number of Stokes's coefficients will always be limited. The maximum degree $nmx \approx 150$ is solved from data of current gravity-dedicated satellite missions. The recovered gravitational potential V is thus represented by values averaged both in space and time. The maximum degree can be translated into spatial resolution (half-wavelength in km)

$$D \; = \; \frac{\pi R}{nmx} \; \doteq \; \frac{20000}{nmx} \; . \tag{16}$$

The gravitational vector in Eq. (9) reads in spherical coordinates

$$\nabla V(r,\theta,\lambda) \; = \; [\; V_r \quad V_\theta \quad V_\lambda \;]^T \; . \tag{17}$$

Entries of the gravitational vector can easily be derived from Eq. (14) by differentiation. Only the radial term having the largest numerical value is presented herein

$$V_r \; = \; h_r^{-1} \; D_r \; V(r,\theta,\lambda) \; = \; - \; \frac{1}{R} \sum_{n=0}^{\infty} \sum_{m=-n}^{n} \; (n+1) \; \left(\frac{R}{r}\right)^{n+2} V_{n,m} \; Y_{n,m}(\theta,\lambda) \; . \tag{18}$$

Entries of the gravitational vector in Cartesian coordinates observed by satellites can be evaluated trough transformation

$$\nabla V(x,y,z) \; = \; \mathbf{J}^T \; \nabla V(r,\theta,\lambda) \; , \tag{19}$$

with the Jacobian $\mathbf{J}$ of transformation between the spherical and Cartesian coordinate systems given by

$$\mathbf{J} \; = \; \nabla \otimes \mathbf{x}(r,\theta,\lambda) \; = \; \begin{bmatrix} \sin\theta \; \cos\lambda & \sin\theta \; \sin\lambda & \cos\theta \\ \cos\theta \; \cos\lambda & \cos\theta \; \sin\lambda & - \; \sin\theta \\ - \; \sin\lambda & \cos\lambda & 0 \end{bmatrix} . \tag{20}$$

Similarly, the gradiometric tensor in Eq. (10) reads in spherical coordinates

$$\mathrm{vec}\,[\; \nabla \otimes \nabla V(r,\theta,\lambda) \;] \; = \; [\; V_{rr} \quad V_{r\theta} \quad V_{r\lambda} \quad V_{\theta\theta} \quad V_{\theta\lambda} \quad V_{\lambda\lambda} \;]^T \; . \tag{21}$$

Some of its entries will directly correspond to observables in the upcoming gradiometric satellite missions. The gradiometric tensor being of rank two has nine entries but only five of them are linearly independent since it is both symmetric and in mass-free space also trace free. Again, the entries of the tensor can easily be derived from Eq. (14) but only the radial component is shown due to its dominant magnitude

$$V_{rr} = h_r^{-2} \; D_r^2 \; V(r,\theta,\lambda) = \frac{1}{R^2} \sum_{n=0}^{\infty} \sum_{m=-n}^{n} \; (n+1) \; (n+2) \; \left(\frac{R}{r}\right)^{n+3} V_{n,m} \; Y_{n,m}(\theta,\lambda) \; . \tag{22}$$

Since spaceborne observations are rather related to the geocentric Cartesian coordinate system, it is also important to find the Cartesian form of the gradiometric tensor

$$\nabla \otimes \nabla V(x,y,z) \; = \; \nabla \otimes \mathbf{J}^T \; \nabla V(r,\theta,\lambda) \; + \; \mathbf{J}^T \; \nabla \otimes \nabla V(r,\theta,\lambda) \; \mathbf{J} \; . \tag{23}$$

Equations (18) and (22) nicely demonstrate how the logarithmic attenuation factor can partially be eliminated by the *sensitivity coefficients* $(n+1) \; r^{-1}$ and $(n+1) \; (n+2) \; r^{-2}$, respectively.

2.3 Geodetic inversion of gravity field parameters

Using an apparatus of Green's surface integrals, the solution of the well-known Dirichlet problem in the potential theory is given by the known *Abel-Poisson integral* that allows for evaluation of the gravitational potential in a general point described by the geocentric radius vector $\mathbf{x}$ external to Lipschitz's boundary (smooth closed surface) on which the gravitational potential is continuously known. The boundary must completely contain all gravitating masses in order to satisfy the Laplace differential equation in the entire solution domain, i.e., everywhere outside the boundary. For the general boundary S described by geocentric radius vectors $\mathbf{y}$, this solution takes a form of the surface integral (Kellogg 1929)

$$\forall \mid \mathbf{y} \mid \leq \mid \mathbf{x} \mid : \; V(\mathbf{x}) = \frac{1}{S} \iint_S V(\mathbf{y}) \; \mathcal{K}(\mathbf{x}, \mathbf{y}) \; dS(\mathbf{y}) \; . \tag{24}$$

Unfortunately, it is not possible to derive the kernel function $\mathcal{K}$ for any general surface S. Due to the shape of the Earth, it is convenient to use the international *reference ellipsoid*. Due to its symmetries, the integral function $\mathcal{K}$ can easily be constructed. It is assumed for the purpose of the solution that all gravitating masses are entirely imbedded inside the reference ellipsoid. The gravitational potential of the external masses (ellipsoidal topography, sea water outside the ellipsoid, atmosphere) is usually accounted for by an appropriate reduction (remove step – direct effect) that is considered to be out of the scope of this text.

Applying in Eq. (24) the operator f at $\mathbf{x}$ yields for the reference ellipsoid S_e

$$\forall \mid \mathbf{y_e} \mid \leq \mid \mathbf{x} \mid : \; f \left[\, V(\mathbf{x}) \, \right] \; = \; \frac{1}{S_e} \iint_{S_e} V(\mathbf{y_e}) \; f \left[\, \mathcal{K}(\mathbf{x}, \mathbf{y_e}) \, \right] \; dS_e(\mathbf{y_e}) \; . \tag{25}$$

Geocentric radius vectors $\mathbf{y_e}$ describe the surface of the reference ellipsoid. The parameter on the left-hand side of Eq. (25) represents an observation taken at the location $\mathbf{x}$ outside the reference ellipsoid and reduced for corresponding effects of all masses outside the reference ellipsoid. On the right-hand side of Eq. (25), one solves for the gravitational potential V distributed over the known ellipsoidal surface S_e with a corresponding surface element dS_e. Their forms depend on the choice of a curvilinear coordinate system related to the reference ellipsoid and discretization of its surface, respectively. Assuming one-parametric *Jacobi ellipsoidal coordinates* defined through the transformations

$$\begin{aligned} u \; &= \; \frac{\sqrt{2}}{2} \sqrt{x^2 + y^2 + z^2 - \varepsilon^2 \; + \; \sqrt{(x^2 + y^2 + z^2 - \varepsilon^2)^2 + \; 4 \, \varepsilon^2 z^2}} \; , \\ \varphi \; &= \; \arctan \frac{u \, \sqrt{x^2 + y^2}}{z \, \sqrt{u^2 + \varepsilon^2}} \; , \\ \lambda \; &= \; \arctan \frac{y}{x} \; , \end{aligned} \tag{26}$$

with radius $0 \le u < \infty$, reduced co-latitude $0 \le \varphi \le \pi$ and longitude $0 \le \lambda < 2\pi$, respectively, the ellipsoidal surface reads

$$S_e = 4\pi a^2 \left(\frac{1}{2} + \frac{b^2}{4a\varepsilon} \ln \frac{a+\varepsilon}{a-\varepsilon} \right) , \tag{27}$$

with the major semi-axis a, minor semi-axis b, linear eccentricity $\varepsilon = \sqrt{a^2 - b^2}$, and

$$dS_e(\varphi, \lambda) = a \sqrt{b^2 + \varepsilon^2 \cos^2 \varphi} \sin\varphi \, d\varphi \, d\lambda . \tag{28}$$

Equation (25) represents the general observation equation for integral inversion of observables represented by the gravitational vector and the gradiometric tensor. Thus, the gravitational vector results in three and the gradiometric tensor in six observation equations, respectively. Outside the gravitating masses, only five equations are linearly independent in the latter case. In both these cases, gravity inversion is an over-determined inverse problem with complicated numerical solutions. Moreover, observation equations and available spaceborne data also allow only for recovery of spectrally-limited values of the unknown gravitational potential; these limitations are related to the logarithmic attenuation of the gravitational field, noise characteristics of data collected in complicated dynamic conditions and their geographically restricted coverage (polar gaps).

2.4 Describing geometry of the gravity field

Besides solving for the gravitational potential V at the known reference surface, geodesy is also interested in estimating the equipotential surface that approximates the mean-sea level: the *geoid*. This concept introduced by C.F. Gauss in 1822 is used in geodesy as a reference surface (vertical datum) in the system of orthometric heights. Vectors $\mathbf{y_g}$ in the geocentric coordinate system can be used to localize the geoid S_g in a 3-D space. By definition, the reference ellipsoid generates the reference gravitational field with the reference ellipsoid being its equipotential surface with the reference potential U equal to the value of the actual potential V (neglecting again the centrifugal component) at the geoid, i.e., $U_e = V_g = \text{const.}$ Then

$$\forall \, | \, \mathbf{y_g} \, | \le | \, \mathbf{x} \, | : \; f \, [\, V(\mathbf{x}) \,] = \frac{U_e}{S_g} \iint_{S_g} f \, [\, \mathcal{K}(\mathbf{x}, \mathbf{y_g}) \,] \; dS_g(\mathbf{y_g}) . \tag{29}$$

The convolution in Eq. (25) disappeared but the integration surface S_g and its surface element dS_g are unknown and should be estimated in terms of the geocentric vectors $\mathbf{y_g}$. The parameter $f(V)$ on the left-hand side of Eq. (29) represents the observed value and the reference gravitational potential U_e at the reference ellipsoid is assumed to be known. At the moment, we also have a vector description of the gravity field in contrary to the scalar description in Eq. (25) in terms of the potential. This is quite natural since the geoid is geometric representation of the gravity field in a 3-D space. We will see that in geodesy one scalar parameter can be used even for its description taking the advantage of the known reference ellipsoid.

Thus, we have formulated two alternative solutions: 1– the gravitational potential V is solved for at the reference ellipsoid S_e, see Eq. (25), and 2– the geoid S_g is solved for in terms of the geocentric vectors $\mathbf{y_g}$ assuming the known value of the gravitational potential at the geoid, i.e., the value of the reference gravitational potential U_e at the reference ellipsoid S_e, see Eq. (29). Perturbation theory is applied to both solutions offering the well known advantage: small numerical values are extracted from erroneous observations increasing significantly the relative accuracy of the resolved parameters. Only deviations of the actual potential V from the reference gravitational potential U called the *disturbing potential* $T = V - U$ is being solved in the former solution. Alternatively, geometric deviations of the geoid from the reference ellipsoid $\Delta\mathbf{y} = \mathbf{y_g} - \mathbf{y_e}$ are estimated in the latter solution. Moreover, the vector description in this solution can be replaced by the distance of the geoid from the reference ellipsoid (geoidal height N) along the ellipsoidal surface normal represented by the unit vector $\mathbf{e_n}$, i.e.,

$$N \;=\; \langle\; \Delta\mathbf{y} \;,\; \mathbf{e_n} \;\rangle \;. \tag{30}$$

Then the transformations in Eqs. (25) and (29) can symbolically be written as follows:

$$f(T) \;\longrightarrow\; T(S_e) \qquad \wedge \qquad f(T) \;\longrightarrow\; N(U_e) \;. \tag{31}$$

The solution represents the disturbing potential T at the surface of the reference ellipsoid, i.e., deviations of the gravitational potential V from the reference potential U at the reference ellipsoid, and/or the geometric deviations N of the geoid from the reference ellipsoid along the ellipsoidal surface normal. Thus, only scalar quantities are solved for in both cases. The functional $f(T)$ in Eq. (31) actually represents observed values that were reduced for the reference field. Once the relationship between the observables and the unknown gravity potential is established (mathematical model), this reduction can easily be performed. The simplest example offers ground gravity as the observable and the gravity disturbance as its reduced form. Equation (31) also demonstrates that both geometry and gravity field of the reference ellipsoid play a very important role in gravity field modeling.

3 Gravity field mapping from space

Using the elementary properties of the Earth's gravity field such as conservativness and irrotationality, its description is possible using the gravity potential. While it cannot be directly observed, ground gravity observations have been collected for more than hundred years. Historically, gravity observations are connected with the names of Galileo Galilei (gravimetry) and Loránd Eötvös (gradiometry). Their contributions honor derived units used in gravimetry (Gal = cm s^{-2}) and gradiometry (Eötvös = s^{-9}), respectively. Most of available data nowadays represent discrete ground gravity observations that have slowly been replaced by airborne data in recent years. However, state-of-the-art techniques in the last six years are related to gravity-dedicated satellite missions. They provide globally distributed spaceborne gravimetric and gradiometric data.

Generally, spaceborne data from gravity-dedicated satellite missions should fulfill the following fundamental criteria:
– uninterrupted tracking in three dimensions;
– measurement or compensation of disturbing effects caused by non-gravitational forces;
– orbital altitude as low as possible;
– sufficient sensitivity to counteract gravity field attenuation.
To meet these requirements, three different concepts of spaceborne gravity field mapping had been proposed: 1– satellite-to-satellite tracking in the high-low mode, 2– satellite-to-satellite tracking in the low-low mode, and 3– satellite gradiometry. All these three concepts were materialized in corresponding missions with two of them orbiting the Earth already. The third mission is under development with a proposed launch date in 2007.

3.1 Satellite-to-satellite tracking in the high-low mode

The concept of satellite-to-satellite tracking in the high-low mode (HL-SST) is relatively simple. An artificial Earth's satellite is equipped with a *Global Positioning System (GPS)* receiver and three-axis *accelerometer (ACC)*. While the orbital trajectory of the satellite is determined accurately through GPS tracking (pseudo-ranges and carrier phases) to the centimeter precision level, the accelerometer at the satellite's centre of mass measures non-gravitational forces such as air drag, Earth's albedo and solar radiation. Generally, the satellite is in a free fall caused mainly by Earth's gravitational pull. Differentiating the estimated trajectory of the satellite in time, its velocity and acceleration vectors can be derived. If reduced for measured effects of non-gravitational forces as well as computed gravitational attraction of other bodies (Moon, Sun, eventually other planets), the gravitational potential can be estimated via fundamental physical laws such as the equation of motion.

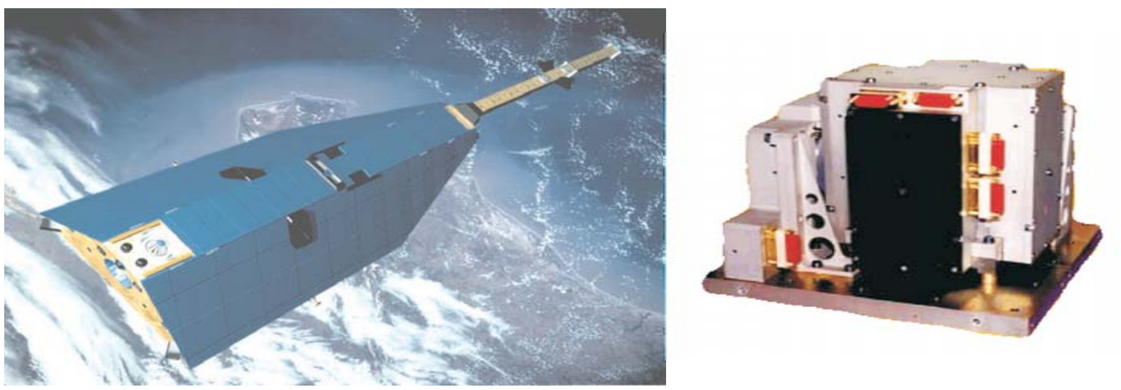

Figure 1: The CHAMP satellite and its accelerometer (Astrium GmbH)

The first satellite of this type, and the first gravity-dedicated satellite mission ever, is the German *Gravity And Magnetic Field Mission CHAMP* (Reigber et al. 2002). Its acronym is originating in the alternative name CHAllenging Minisatellite Payload. The CHAMP satellite was launched on July 15, 2000 into an almost circular, near polar orbit (inclination of 87 arcdeg) with an initial altitude of 454 km. The reason for choosing an almost circular and near-polar orbit is the advantage of getting a homogeneous and almost complete global coverage of the Earth's sphere with orbit to resolve the gravitational potential. The relatively high initial altitude was chosen to guarantee a multi-year mission duration even under severe solar activity conditions. The initial design lifetime of the satellite system (five years) was extended at least for another two years.

In the accelerometer, a proof-mass is floating freely inside a cage supported by an electrostatic suspension. The cavity walls are equipped with the electrodes that control the motion (both translation and rotation) of a proof-mass by electrostatic forces. By applying a closed-loop control inside the sensor unit, the proof-mass is kept motionless in the center of the cage. The detected acceleration is then proportional to the forces needed to fulfill this task. The CHAMP satellite also carries the laser retro-reflector that allows to measure direct two-way ranges between a ground station and the satellite with a single-shot accuracy of 1-2 cm without any ambiguities. These data are used for precise orbit determination in connection with GPS. Two advanced stellar compasses provide high precision attitude information for all instruments fixed to the spacecraft body.

The primary science objective of the CHAMP mission is to provide highly precise global long-wavelength features of the static Earth's gravity field and its temporal variations. CHAMP thus contributes to investigations of the structure and dynamics of the solid Earth from the core along the mantle to the crust, and of interactions with the ocean and atmosphere. Besides the gravity field research, additional on-board instrumentation allows for mapping the main and crustal magnetic fields of the Earth including their space/time variability, and for global estimation of temperature, water vapor and electron content within the atmosphere and ionosphere.

The CHAMP mission has one major advantage of being relatively simple, thus also relatively inexpensive. Other two observation techniques discussed in next subsections are more complicated involving either two satellites or more sophisticated instrumentation. From this perspective, CHAMP was an ideal candidate for a pioneer gravity-dedicated satellite mission. However, it does not comply to the fourth criterion required for gravity-dedicated satellite missions: sufficient sensitivity to small features of the gravity field. The classical approach of highlighting or emphasizing small features in physics – differentiation – is first applied in the next two concepts. For the gravity field, CHAMP commenced the international decade of global gravity models. Although the two follow-up missions supersede CHAMP in terms of both accuracy and resolution of derived gravity field models, its observation technique (HL-SST) helps to de-correlate estimated Stokes's coefficients and makes in such a way current gravity field models much more reliable.

3.2 Satellite-to-satellite tracking in the low-low mode

For satellite-to-satellite tracking in the low-low mode (LL-SST), two identical spacecraft essentially in the same orbit and at a distance of few hundreds of km apart chase each other (Wolff 1969). The relative motion of the satellites is measured with the highest possible precision. Effect of non-gravitational forces can once again either be measured or compensated for. Observed data – namely those related to the relative motion of the satellites – can be used for deriving acceleration differences of the two satellites along their line-of-sight. Through the equation of motion, these differences can directly be linked to corresponding gradient differences of the gravitational potential. The two satellites can theoretically be seen as a large 1-D gradiometer.

The first experiment of this type is the US-German satellite mission *Gravity Recovery And Climate Experiment (GRACE)* launched on March 17, 2002 (Tapley et al. 2004). The mission consists of two identical spacecraft following each other along almost circular, low and polar orbit (inclination of 89 arcdeg). The GRACE satellites fly 220 ± 50 km apart. During the five-year lifetime of the mission, the relative motion of the two satellites is measured using a very sensitive *K-band ranging system (KBR)* that senses changes in separation between the two satellites. Moreover, the GRACE satellites are also equipped with geodetic quality GPS receivers allowing for accurate orbit determination and accelerometers measuring a sum of all non-gravitational forces affecting the satellites. The GRACE mission is thus based on satellite-to-satellite tracking in both the low-low and high-low mode.

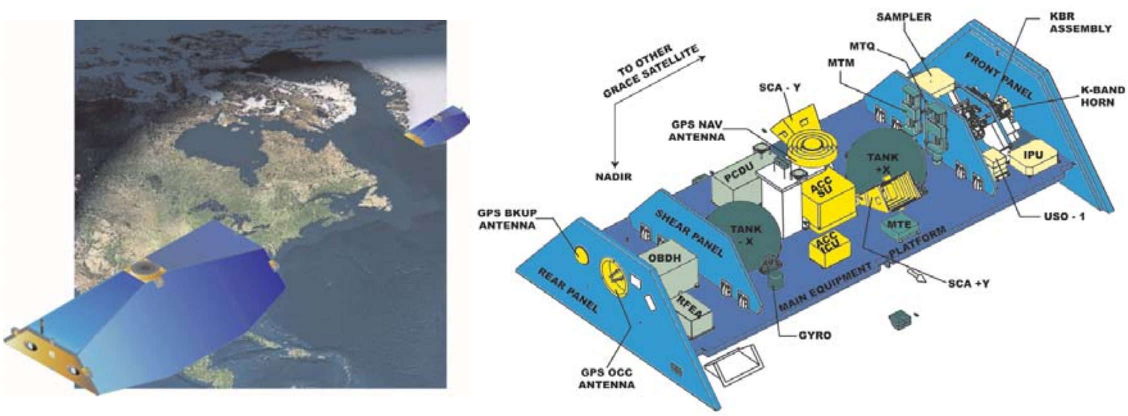

Figure 2: The GRACE satellites and their anatomy (GFZ Potsdam)

The accuracy increase with respect to CHAMP is achieved by a K-band microwave link that measures the exact separation distance and its rate of change to an accuracy of better than 1 μm s^{-1}. To consider precise attitude and non-gravitational forces, both satellites are again equipped with star cameras and accelerometers. The position and velocity of the satellites are measured using on-board GPS receivers. The GRACE satellites could be seen as two CHAMP satellites equipped additionally with the microwave ranger.

The primary science objective of the GRACE mission is to provide precise global and high-resolution estimates of the static and time-variable part of the Earth's gravity field. It is namely the long-wavelength component of the field and its temporal variations (monthly solutions) that are being solved from the GRACE SST data. Additionally, GPS measurements and its derived quantities of temperature and water vapor contribute to climate variability studies and improved resolution of the fine structure of the ionosphere. Estimates of time variable components of the gravity field helps for a better understanding of time variable processes in oceanography, hydrology, glaciology or solid Earth sciences.

3.3 Satellite gradiometry

The satellite gradiometry is based on measuring second-order directional derivatives of the gravitational potential improving further the sensitivity of observed data to small features in the gravitational field. At the moment (January 2007) there is no gradiometric mission in operation. The first gradiometric mission is under development. The *Gravity field and steady-state Ocean Circulation Explorer (GOCE)* satellite will have a small cross section of approximately 0.9 m^2, and will be totally symmetrical to minimize the influence of non-gravitational forces (Drinkwater et al. 2003). There will be no moving parts or mechanisms to produce shocks. There will also be no sloshing effects as all the thruster fuel is gas. The actuators for the orbit maintenance and along-track drag control is a pair of ion thrusters. Smaller, proportional micro-thrusters are used for attitude control.

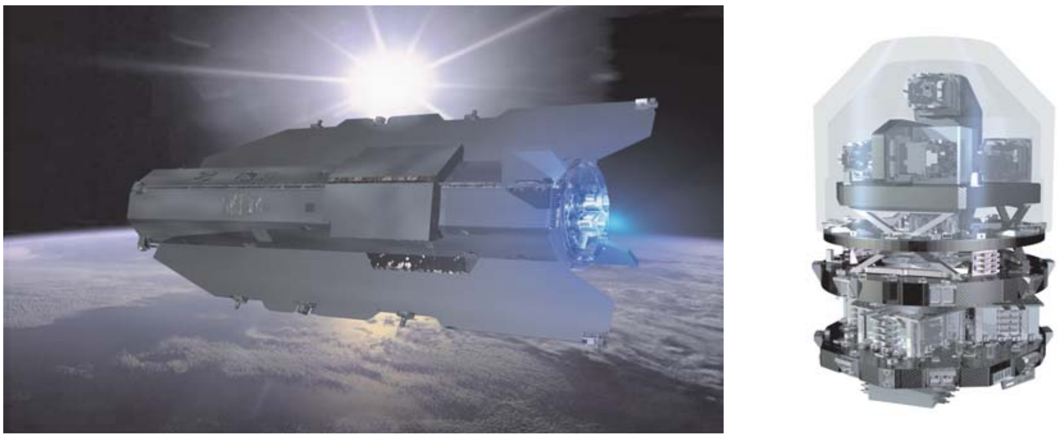

Figure 3: The GOCE satellite and its gradiometer (ESA)

GOCE will employ a three-axis *electrostatic gravity gradiometer (EGG)* that will allow for the first time gravity gradients to be measured in all spatial directions. It is designed specifically for determining the stationary gravity field. The measured signal is the difference in gravitational acceleration at the proof-mass location inside the spacecraft caused by mass anomalies within the Earth. Exploiting these differential measurements for all three spatial axes has the advantage that all disturbing forces acting uniformly on the spacecraft, e.g., drag, thrusters resulting in linear or angular acceleration, can be compensated for. The length of the baseline for an accelerometer pair is 0.5 m and its noise within the measurement bandwidth is smaller than 3 mE = 3 $\times 10^{-12}$ s^{-2}. It is namely the extreme accuracy of the gradiometer that is expected to further improve gravity field models, namely their medium-wavelength portion. The noise at the mE level corresponds approximately to acceleration of aircraft carrier colliding with a snowflake.

The main final geophysical product will be a global gravity field expressed as a set of coefficients where the gravitational potential is described with a spherical harmonic expansion. The primary objective of GOCE is the provision of high-accuracy and high-resolution models for the static part of the Earth's gravity field. It is namely the medium-wavelength part of the field that should complement the long-wavelength model based on the GRACE data. Due to the short duration of the mission, temporal variations will not be estimated in this case.

All three satellite missions are compared in terms of selected parameters in Table 1:

	CHAMP	GRACE	GOCE
altitude (km)	454	485	250
orbital inclination (arcdeg)	87,3	89,5	96,5
orbital eccentricity	0,004	0,001	0,005
orbital period (min)	93	95	< 30
initial mass (kg)	522	2×485	1100
launch (month/year)	07/00	03/02	09/07
sensitivity (maximum degree)	50	100	200
payload for gravity recovery	ACC/GPS	ACC/GPS /KBR	GPS/EGG
mission duration (month)	60	60	24
institution	GFZ	NASA/GFZ	ESA

Table 1: Selected parameters of current gravity dedicated satellite missions

4 Mathematical models

The problem of gravity field modeling based on spaceborne data was briefly outlined in Section 2. Generally, we look for a mathematical model that would relate available spaceborne observables to the unknown values, namely the Stokes coefficients of the gravitational potential $V_{n,m}$. According to transformations in Eq. (31), scalar-valued perturbations of the gravitational potential and geometric deviations of the geoid from the selected model (reference ellipsoid and its gravitational potential) can also be solved for (perturbation theory at work).

The link between observations $f(V)$ reduced for the effect of the reference potential $f(U)$ and the unknown parameter T can be established as follows :

$$\forall \mid \mathbf{y_e} \mid \leq \mid \mathbf{x} \mid : \; f \,[\, T(\mathbf{x}) \,] \;=\; \frac{1}{S_e} \iint_{S_e} T(\mathbf{y_e}) \; f \,[\, \mathcal{K}(\mathbf{x}, \mathbf{y_e}) \,] \;\; dS_e(\mathbf{y_e}) \; . \tag{32}$$

This equation originates in Eq. (25) reducing both sides for the reference parameter

$$\forall \mid \mathbf{y_e} \mid \leq \mid \mathbf{x} \mid : \; f \,[\, U(\mathbf{x}) \,] \;=\; \frac{U_e}{S_e} \iint_{S_e} f \,[\, \mathcal{K}(\mathbf{x}, \mathbf{y_e}) \,] \;\; dS_e(\mathbf{y_e}) \; . \tag{33}$$

This is the well known and in geodesy often used reduction of gravity field observables for the reference potential. Depending on the mathematical model, this reduction may be more or less complicated. Having a mathematical description of the reference potential (Pizzetti 1911) and knowing the operator f, the reduction can easily be derived.

In order to keep this theoretical section short, mathematical models for inversion of the GRACE SST data are only outlined in the next subsection. The GRACE data have some unique features due to combination of spaceborne gravimetric and gradiometric approaches. Thus, they provide a good example for other spaceborne gravity data discussed in this text.

4.1 Inverting data of type GRACE

For the GRACE mission, position, velocity and acceleration vectors of both satellites in the geocentric Earth-fixed coordinate system, i.e.,

$$\mathbf{x} = [\; x \quad y \quad z \;]^T \;, \qquad \dot{\mathbf{x}} = [\; \dot{x} \quad \dot{y} \quad \dot{z} \;]^T \;, \qquad \ddot{\mathbf{x}} = [\; \ddot{x} \quad \ddot{y} \quad \ddot{z} \;]^T \;, \tag{34}$$

can be derived from GPS code and carrier beat phase observations. The first- and second-order time derivatives are identified by a dot and by a double dot, respectively. The space segment of the GRACE mission consists of two satellites following each other along a similar orbit. Let us assign the leading satellite with the index 1 and the trailing satellite with the index 2. Positions of the satellites and their derivatives will be then labeled with corresponding indices. An operator δ for differences between functions corresponding to the positions of the two satellites is used throughout the subsection. Vector differences between the two satellites in position, velocity and acceleration are then given as follows:

$$\delta\mathbf{x} \;=\; \mathbf{x}_2 \;-\; \mathbf{x}_1 \;, \qquad \delta\dot{\mathbf{x}} \;=\; \dot{\mathbf{x}}_2 \;-\; \dot{\mathbf{x}}_1 \;, \qquad \delta\ddot{\mathbf{x}} \;=\; \ddot{\mathbf{x}}_2 \;-\; \ddot{\mathbf{x}}_1 \; . \tag{35}$$

The LL-SST provides the *inter-satellite range*, e.g., (Blaha 1992),

$$\varrho \;=\; \sqrt{< \delta\mathbf{x} \mid \delta\mathbf{x} >} \;=\; \mid \delta\mathbf{x} \mid \;\; . \tag{36}$$

Considering the unit vector of the inter-satellite direction (line-of-sight)

$$\mathbf{e} \;=\; [\; e_x \quad e_y \quad e_z \;]^T \;=\; \frac{\delta\mathbf{x}}{\varrho} \;, \tag{37}$$

the LL-SST data can be used for derivation of the first-order time derivative of the range called herein *inter-satellite velocity*

$$\dot{\varrho} \;=\; <\delta\dot{\mathbf{x}} \mid \mathbf{e}> + <\delta\mathbf{x} \mid \dot{\mathbf{e}}> \;=\; <\delta\dot{\mathbf{x}} \mid \mathbf{e}> \,, \tag{38}$$

as well as of the second-order time derivative called herein *inter-satellite acceleration*, e.g., (Rummel 1980),

$$\ddot{\varrho} \;=\; <\delta\ddot{\mathbf{x}} \mid \mathbf{e}> + <\delta\dot{\mathbf{x}} \mid \dot{\mathbf{e}}> \;=\; <\delta\ddot{\mathbf{x}} \mid \mathbf{e}> \;+\; \frac{\mid \delta\dot{\mathbf{x}} \mid^2 \;-\; \dot{\varrho}^2}{\varrho} \,. \tag{39}$$

Above mentioned SST data are provided by several sensors on board of the GRACE satellites. The HL-SST data are measured by the Black Jack GPS receivers. Raw GPS data (code and carrier beat phase observations) are processed in order to recover the position and velocity vectors of the GRACE satellites in the terrestrial (Earth-fixed) coordinate system. The acceleration vector is obtainable by numerical differentiation from the velocity vector rotated to the celestial (non-rotating) coordinate system. So-called kinematic orbits are generated by analysis centers responsible for processing GRACE data. They are usually computed at the sampling rate of 30 seconds with the accuracy at the level of 5 cm. The LL-SST data are obtained from the K-band ranging system. They can be found among data supplied by the GRACE data centers at the Jet Propulsion Laboratories and GeoForschungsZentrum. The inter-satellite range can be derived with the total error of 10 μm at the sampling rate of 0.2 Hz. Moreover, the GRACE satellites are also equipped with SuperSTAR accelerometers. Non-gravitational acceleration can be derived with the precision of 100 μGal at the sampling rate of 0.1 Hz. The most significant non-gravitational forces affecting the motion of the GRACE satellites are the atmospheric drag and solar pressure radiation, see, e.g., (Montenbruck and Gill 2001). The data from the on-board sensors considered for formulation of a mathematical model thus represent time series of the position, velocity and acceleration vectors, inter-satellite ranges and their time derivatives, and vectors of non-gravitational acceleration, respectively. The argument of time will be omitted in the following text referring our derivations to a single epoch. It is acknowledged that effects computed from various geophysical models (various tidal and loading effects) must also be considered for deriving a complete model. Namely high-frequency variations of the gravitational field must be modelled to avoid aliasing errors.

In the inertial reference frame, acceleration of a unit-mass satellite can be expressed according to Newton's law of motion as follows:

$$\ddot{\mathbf{x}} \;=\; -\; \nabla V(\mathbf{x}) \,. \tag{40}$$

The inertial frame is approximated by the non-rotating geocentric celestial frame. The transformation between the terrestrial and celestial frames is well known (McCarthy and Petit 2004). Since all vectors can easily be transformed between the two frames, no new notation is introduced herein. It is obvious that the vector quantities must be related to the same coordinate system when used in the same equation. Only the gravitational effect of the Earth's masses is considered in Eq. (40). The inter-satellite acceleration vector of the GRACE satellites can be then written

$$\delta \ddot{\mathbf{x}} \; = \; - \, \delta \nabla V(\mathbf{x}) \; . \tag{41}$$

Combining Eqs. (39) and (41), the observation equation for the GRACE observables can be written in the form

$$\mid \delta \dot{\mathbf{x}} \mid^2 \; - \; \dot{\varrho}^2 \; - \; \varrho \, \ddot{\varrho} \; = \; < \delta \nabla V(\mathbf{x}) \mid \delta \mathbf{x} > \; . \tag{42}$$

This equation can be considered as an observation equation for the SST data of type GRACE. The equation is not complete as was indicated above: additional terms must be included in real data analysis (non-gravitational and geophysical effects).

Equation (42) can be solved in the *spectral form* by its combination with Eqs. (17) and (19). The unknown parameters in this case are the Stokes coefficients $V_{n,m}$. Their number must be limited by some maximum degree nmx. For the GRACE mission $nmx \approx 150$. The obtained observation equation is linear with respect to the unknown parameters, thus no other modifications must be done. Still, the large number of both observations and unknowns create many problems for numerical solutions.

Alternatively, the unknown gravitational potential can be solved in the *spatial form*. In this case, Eqs. (25) and (42) are considered. Replacing the reference ellipsoid by a geocentric sphere $S_r : \mid \mathbf{y_r} \mid = R$, their combination results in the integral form of the observation equation (Novák et al. 2006)

$$\mid \delta \dot{\mathbf{x}} \mid^2 \; - \; \dot{\varrho}^2 \; - \; \varrho \, \ddot{\varrho} \; = \; \frac{1}{S_r} \iint_{S_r} V(\mathbf{y_r}) \; \mathcal{H}(\mathbf{x}_1, \mathbf{x}_2, \mathbf{y_r}) \; dS_r(\mathbf{y_r}) \; , \tag{43}$$

with the scalar three-point kernel function

$$\mathcal{H}(\mathbf{x}_1, \mathbf{x}_2, \mathbf{y_r}) \; = \; < \delta \nabla \mathcal{K}(\mathbf{x}, \mathbf{y_r}) \mid \delta \mathbf{x} > \; . \tag{44}$$

For a single epoch, the integral kernel $\mathcal{H}$ relates the gravitational potential V at the spherical surface S_r with the functional on the left-hand side of Eq. (43) derived from the SST data of type GRACE. This makes the kernel function $\mathcal{H}$ different from typical integral kernels used in geodesy that usually relate only two points such as the Stokes, Hotine or Vening-Meinesz functions. The quadrature of the surface integral can be used for its numerical evaluation, i.e.,

$$\frac{1}{S_r} \iint_{S_r} V(\mathbf{y_r}) \; \mathcal{H}(\mathbf{x}_1, \mathbf{x}_2, \mathbf{y_r}) \; dS_r(\mathbf{y_r}) \; \approx \; \frac{1}{4\pi} \sum \overline{V}(\mathbf{y_r}) \; \mathcal{H}(\mathbf{x}_1, \mathbf{x}_2, \mathbf{y_r}) \; \Delta S_r \; . \tag{45}$$

The solution of Eq. (45) is then given in terms of surface mean values of the function V that correspond to normalized discrete surfaces $\Delta S_r = \sin\theta \; \Delta\theta \; \Delta\lambda$. If applied correctly, the spectral and spatial solutions should be identical: the harmonic analysis of computed mean values of the function V should provide the Stokes coefficients $V_{n,m}$ and vice versa.

Let us look now at the gradiometry with GRACE (Keller and Hess 1998). Assuming the satellites are identical, the radius vector of their barycenter B is estimated as follows:

$$\mathbf{x}_B = \frac{\mathbf{x}_1 + \mathbf{x}_2}{2} . \tag{46}$$

The gravitational potential at the first satellite can be related to the barycenter

$$\nabla_1 V(\mathbf{x}) \doteq \nabla_B V(\mathbf{x}) + \nabla_B \otimes \nabla_B V(\mathbf{x}) \; (\mathbf{x}_1 - \mathbf{x}_B) , \tag{47}$$

while only the linear term of the expansion series was considered. Similarly,

$$\nabla_2 V(\mathbf{x}) \doteq \nabla_B V(\mathbf{x}) + \nabla_B \otimes \nabla_B V(\mathbf{x}) \; (\mathbf{x}_2 - \mathbf{x}_B) . \tag{48}$$

Keeping the linear approximation in mind, subtracting Eq. (47) from Eq. (48) yields

$$\delta \nabla V(\mathbf{x}) = \nabla_B \otimes \nabla_B V(\mathbf{x}) \; \delta\mathbf{x} . \tag{49}$$

Substituting Eq. (49) into Eq. (42) yields the gradiometric observation equation

$$| \, \delta\dot{\mathbf{x}} \, |^2 - \dot{\varrho}^2 - \ddot{\varrho} \; \varrho = < \nabla_B \otimes \nabla_B V(\mathbf{x}) \; \delta\mathbf{x} \; | \; \delta\mathbf{x} > . \tag{50}$$

Combining Eqs. (25) and (50) then results in the spatial form (Novák et al. 2006)

$$| \, \delta\dot{\mathbf{x}} \, |^2 - \dot{\varrho}^2 - \ddot{\varrho} \; \varrho = \frac{1}{S_r} \iint_{S_r} V(\mathbf{y_r}) \; \mathcal{G}(\mathbf{x}_B, \mathbf{y_r}) \; dS_r(\mathbf{y_r}) , \tag{51}$$

with the scalar-valued two-point kernel function

$$\mathcal{G}(\mathbf{x}_B, \mathbf{y_r}) = < \nabla_B \otimes \nabla_B \; \mathcal{K}(\mathbf{x}, \mathbf{y_r}) \; \delta\mathbf{x} \; | \; \delta\mathbf{x} > . \tag{52}$$

In this case, only the barycenter of the GRACE satellites and the computation point are related through the integration kernel $\mathcal{G}$. Even Eq. (50) can be solved in the spectral form by expanding the function V into the spherical harmonic series.

Equations (42) and (50) represent two observation equations relating the SST data of type GRACE to the unknown gravitational potential. In the first equation, the potential gradient difference is used while the second equation contains the full gradiometric tensor (matrix direct product of the gradient). The surface integrals in Eqs. (43) and (51) can be evaluated without problems related to the eventual singularity of the respective integral kernels. Moreover, the series representation of the kernel functions will always be degree-limited.

5 New gravity models and their applications

Prior to the CHAMP and GRACE missions, the long-wavelength part of the Earth's gravity field from spaceborne data was determined from various tracking measurements of a greater number of satellites. Unfortunately, these data were of varying quality and restricted by geographical coverage. Consequently, the accuracy and spatial resolution of derived gravity field models were limited with most of the satellite contributions restricted to wavelengths of 1000 km or longer. At shorter wavelengths, the errors were too large to be useful. Thus, improvements to gravity models at medium and short wavelengths had to come from the use of ground, marine and airborne gravity measurements. However, they are also of varying vintage, quality and geographic coverage. Due to the restricted access to observed data, global gravity models were also produced only by a limited number of research teams.

The situation changed dramatically with the launch of the CHAMP and GRACE satellites. After some initial testing phase, their observed data became available to various research groups worldwide. Consequently, a series of new global gravity models has been released. Already the first results based on preliminary analysis of short spans of observed data showed significant advances in both the accuracy and resolution of the recovered gravity models. Figure 4 depicts the anomalous gravity field based on decades of pre-CHAMP and pre-GRACE data compared to the model based only on 110 days of GRACE observations. The improvement in the resolution of the gravity model (units of mGal) is clearly visible.

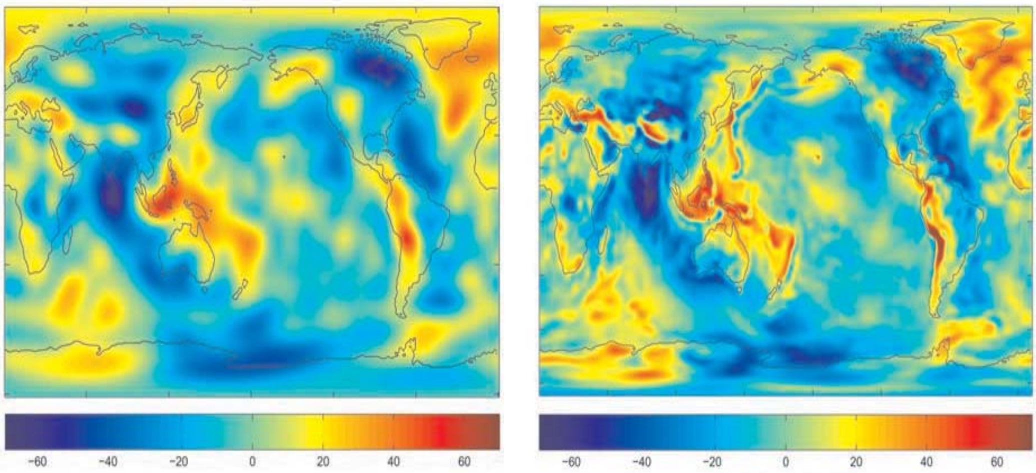

Figure 4: Pre-GRACE vs. GRACE-based gravity models (GFZ Potsdam)

Due to a large involvement of the GeoForschungsZentrum (GFZ) Potsdam, German research centre for geosciences, in both missions, only their results are briefly summarized herein. Other teams have contributed in this field but it is out of the scope of this text to list all of them. GFZ results are used to document the recent progress in accuracy and resolution of the new global gravity models. Based on the CHAMP SST data, a series of gravity field models was computed: starting with EIGEN-1S, the first model including CHAMP data, up to EIGEN-CHAMP03S derived from 33 months of data. The estimated accuracy of the latest model EIGEN-CHAMP03S is about 5 cm and 0.5 mGal in terms of the geoidal height and gravity, respectively, for spatial resolution of $D = 400$ km.

The first GRACE gravity model EIGEN-GRACE01S was released in July 2003. The model based on 39 days of preliminary GRACE flight instrument data gathered in August and November 2002 was about 5 times more accurate than the latest CHAMP field and about 50 times more accurate than the best pre-CHAMP satellite-only gravity model for spatial resolution of $D = 1000$ km. The medium-wavelength gravity field model EIGEN-GRACE02S was calculated from 110 days of the GRACE tracking data. This model fully independent from oceanic and continental surface gravity data was derived solely from SST data of GRACE. It resolves the geoid with the accuracy of better than 1 mm at spatial resolution of $D = 1000$ km, i.e., it is about one order of magnitude more accurate than then CHAMP-based global gravity models and more than two orders of magnitude more accurate than the latest pre-CHAMP satellite-only gravity model GRIM5-S1. The accuracy of gravity models based on pre-CHAMP, CHAMP and GRACE data in terms of the accumulated error in the geoidal height is compared in Figure 5.

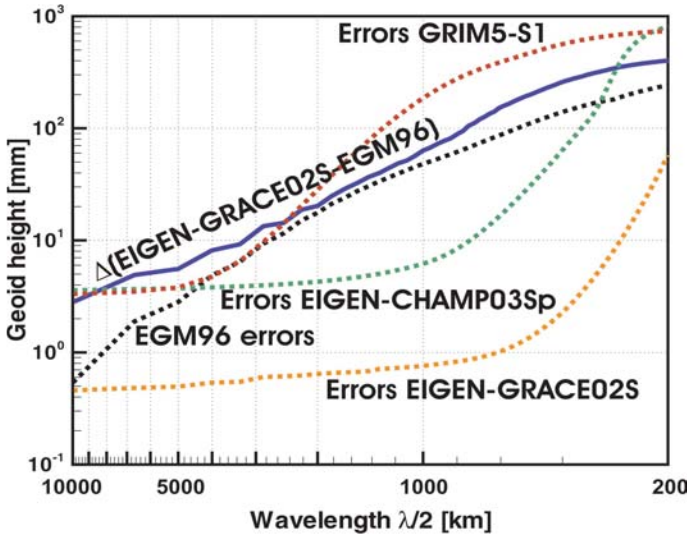

Figure 5: Accuracy of the geoid vs. spatial resolution (GFZ Potsdam)

5.1 Geodesy

The global geoid estimated with centimeter accuracy and global gravity model with 1-2 mGal accuracy at about 100 km spatial resolution, such as expected from combination of GRACE and GOCE SST data, would also serve some fundamental geodetic applications; among them the most important ones are:

1. Leveling with GPS. With the aid of geoidal heights above the reference ellipsoid, any geometric heights determined by GPS or any follow-on system, are convertible to heights above sea-level. These physical heights still keep their importance since they indicate what is up and down throughout science and engineering. This new technique will revolutionize height determination and make it much less time consuming and expensive.

2. Unification of height systems. There are still a large number of unconnected height systems around the world. Each system refers to a reference point, usually a benchmark close to the sea and connected by leveling to mean sea-level obtained by a tide gauge. The discontinuity in height systems is of no importance as long as there is no requirement to compare height values from the various systems. In the past, discontinuities had to be accepted whenever different geographical areas (with their individual height systems) were separated by sea. With the new accurate geoid, it will be possible to connect all height systems with centimeter precision, provided at least one benchmark in each height system is equipped with some space positioning technique such as GPS.

3. Inertial navigation. A principle of inertial navigation is quite simple: accelerometers measure motion of some moving platform and single and double integration yields its velocity and position differences. Changes in the orientation of the accelerometer triad are taken into account by gyros. However, one fundamental source of error is that the accelerometers measure not only motion of the platform, but the sum of its kinematic and gravity acceleration. At present, the gravity part is taken into account via the ellipsoidal gravity model. As a consequence, deviations of the actual and ellipsoidal gravity field are interpreted erroneously as platform accelerations. Precise knowledge of the gravity field will drastically reduce this source of error.

4. Orbit determination. New accurate gravity field models will provide a significant improvement in orbit computations for all Earth-orbiting satellites. They will lead to a better understanding of physics behind orbit perturbations. Especially for low-orbiting satellites, such models will enable separation of perturbations due to the static gravity field and those due to other perturbing forces. The latter do not only include non-conservative forces caused by air drag and solar radiation, but also perturbations caused by the solid Earth and ocean tides. It is foreseen that some significant improvements can be made in modeling these perturbations.

5.2 Solid Earth and oceanography

As in the case of other planets, the gravity field of the Earth is an essential quantity for probing its interior structure and for modeling of its dynamical behaviour under various circumstances, such as heating from the interior, redistribution of masses between solid and fluid parts, and loading of its surface.

In *solid-Earth physics* the production of the gravity field model is not the primary goal. It rather aims at the provision of a detailed 3-D image of density variations in the lithosphere and upper mantle, as derived from a combination of gravity, seismic tomography, lithospheric magnetic-anomaly information and topographic models. The density information then allows for precise quantitative modeling of sedimentary basins, rifts, tectonic motions and sea/land vertical changes. The latter is of particular importance for estimation of global sea-level variations. Further, the density contributes significantly to the better understanding of the occurrence of subcrustal earthquakes, a long-standing geophysical modeling objective which will lead to significantly improved quantification of various seismic hazard risks.

In *oceanography*, the mean dynamic ocean topography derived from the new global geoid in combination with precise altimetry, will allow for determination of practically all ocean current systems in terms of location and amplitude, from the strongest through to the weaker deep-ocean and coastal current systems. In particular, knowledge of the marine geoid with centimeter accuracy and spatial resolution at the level of $D = 100$ km or better will ensure:

– mapping of short-wavelength features of the dynamic topography to 1-2 cm accuracy on a global basis;

– notification of practically all features within the mean geostrophic current field by the improved knowledge of the dynamic topography;

– better understanding of the role of the positions, strengths and dynamics of the short-spatial scale fronts and jets in controlling and influencing the ocean circulation;

– significant reduction in oceanic transport and global ocean heat budget uncertainties.

Each area of application for the new gravity models has specific accuracy requirements that are summarized in terms of geoidal heights and gravity in Table 2:

Application	accuracy geoid (cm)	accuracy gravity (mGal)	resolution (km)
Geodesy :			
leveling by GPS	1		100-1000
unification of height systems	1		100-20000
inertial navigation		$\sim$ 1-5	100-1000
orbit determination		$\sim$ 1-3	100-1000
Solid Earth :			
upper-mantle density		1-2	100
continental lithosphere :			
– sedimentary basins		1-2	50-100
– rifts		1-2	20-100
– tectonic motions		1-2	100-500
– seismic hazards		1	100
oceanic lithosphere		0.5-1	100-200
Oceanography :			
short-scale	1-2 / 0.2		100 / 200
basin scale	$\sim$ 0.1		1000

Table 2: Accuracy and resolution requirements for different applications

6 Conclusions

The new gravity-dedicated satellite missions discussed in this lecture have been providing high-quality tracking data that can be used for production of new global models of the Earth's gravity field. These geodetic products including the static field and its temporal variations are of both unprecedented accuracy and spatial resolution. Combining the low-low satellite-to-satellite tracking data (GRACE) with spaceborne gradiometric data (GOCE), the static gravity field should be resolved with the accuracy of 1 mGal for spatial resolution (half-wavelength) of 100 km. Geometry of the gravity field in terms of the geoid should be known for identical resolution with the accuracy of 1 cm. Besides the static field, its temporal variations are also estimated. Namely the GRACE mission contributes to this task allowing for recovery of monthly solutions. Although their spatial resolution is smaller than that of the static field, their analysis will still allow for a large number of investigations related to mass shifts within the solid Earth, oceans and atmosphere. It can be expected that spaceborne data from these satellite missions either already collected or still to be gathered within the next years will introduce a new area of multi-disciplinary research in solid Earth physics, oceanography, and geodesy itself.

In view of recent changes of global climate and various natural disasters affecting people around the world with an increasing frequency, these new geodetic products are of a great importance. They help researchers in different geosciences to understand better the full complexity of the Earth's system and interactions of its various components. They are already now many phenomena, that can be studied through the new gravity field models, and new are still emerging. Sea-level changes, changes in ocean circulation, volume, temperature and salinity, solid mass movements, ice mass changes – all these phenomena influence our everyday life. To support the sustainable development of the entire human society and to protect its living environment, the reliable knowledge of all these processes will be extremely important.

For the geodetic community, the current era is very exciting with instrumentation providing excellent observational material that is moreover available to all interested parties. Thus, even the Czech geodesy, having some excellent record in this field starting with the first published estimation of the Earth's flattening based solely on spaceborne data of the first artificial Earth's satellite Sputnik by Prof. Emil Buchar in 1957, has the opportunity to contribute to these efforts. It is namely the duty of current and future academic staff to get talented students involved in the geodetic science – one of the oldest scientific disciplines.

Acknowledgement: This study was supported by the grant No. 205/05/2777 of the Czech Science Foundation, and by the research plans No. MSM4977751301 and LC506 of the Czech Ministry of Education, Youth and Sports.

References

Abramowitz M, Stegun CA (1972) *Legendre functions.* Handbook of mathematical functions with formulas, graphs and mathematical tables. Dover, New York.

Blaha G (1992) Refinement of the satellite-to-satellite line-of-sight acceleration model in a residual gravity field. *Manuscripta Geodaetica* 17: 321-333

Drinkwater MR, Floberghagen R, Haagmans R, Muzi D, Popescu A (2003) GOCE: ESA's first Earth Explorer Core mission. *Space Sciences Series of ISSI* 18 (Earth Gravity Field from Space – from Sensors to Earth Sciences): 419-432

Heiskanen WA, Moritz H (1967) *Physical geodesy.* Freeman and Co., San Francisco.

Hobson EW (1931) *The theory of spherical & ellipsoidal harmonics.* Chelsea, New York.

Keller W, Hess D (1998) Gradiometrie mit GRACE. *Zeitschrift für Vermessungswesen* 124: 137-144

Kellogg OD (1929) *Foundations of potential theory.* Springer, Berlin.

McCarthy DD, Petit G (2004). IERS Conventions (2003) IERS Technical Note 32. Verlag des Bundesamtes für Kartographie und Geodäsie, Frankfurt am Main.

Montenbruck O, Gill E (2001) Satellite orbits. Model, methods, applications. Springer Berlin Heidelberg New York.

Novák P, Austen A, Sharifi MA, Grafarend EW (2006) Mapping Earth's gravitation using GRACE data. In: *Observation of the Earth System from Space.* Springer Berlin Heidelberg New York, ISBN: 3-540-29520-8

Pizzetti P (1911) Sopra il Calcolo Teorico delle Deviazioni del Geoide dall' Ellisoide. *Atti Reale Accademia delle Scienze* 46, Torino.

Reigber C, Luehr H, Schwintzer P (2002) CHAMP mission status. *Advances in Space Research* 30: 129-134

Rummel R (1980) Geoid heights, geoid height differences, and mean gravity anomalies from low-low satellite-to-satellite tracking – an error analysis. Report No. 409, Department of Geodetic Science and Surveying, Ohio State University, Columbus.

Tapley BD, Bettadpur S, Watkins M, Reigber C (2004) The gravity recovery and climate experiment: mission overview and early results. *Geophysical Research Letters* 31: 1-6

Wolff M (1969) Direct measurement of the Earth's gravitational potential using a satellite pair. *Journal of Geophysical Research* 74: 5295-5300

Curriculum vitae

Pavel Novák $\ast$ 21.09.1965 Plzeň, Czech Republic

Education and qualification

1989 Master of Science, Czech Technical University in Prague, Czech Republic
1996 Doctor of Philosophy, University of New Brunswick in Fredericton, Canada
2003 Associate Professor, Czech Technical University in Prague, Czech Republic

Professional positions

1991 – 1992 Technical University Berlin, research associate
1992 – 1996 Research Institute of Geodesy, Topography and Cartography, researcher
1996 – 1999 University of New Brunswick (UNB), PhD student and research associate
1999 – 2001 The University of Calgary, research associate
2001 – Research Institute of Geodesy, Topography and Cartography, researcher
2002 – 2004 University of Stuttgart, research associate
2004 – University of Western Bohemia (UWB), associate professor

Teaching activities

geodesy 1 (UNB 1996), geodesy 2 (UNB 1997, 1999), geodesy 3 (UNB 1996, 1997, 1998), adjustment calculus (UNB 1997, 1998, 1999), surveying for civil engineers (UNB 1999), surveying camps (UNB 1997, 1998), introduction to the Earth's gravity field (UWB 2003), global positioning systems (UWB 2004, 2005, 2006), advanced geodesy (UWB 2004, 2005, 2006), geodetic methodology (UWB 2006)

Membership in professional associations and activities

international editorial board of the Journal of Geodesy, Subcommission on Geosciences of the Czech Science Foundation, International Association of Geodesy (IAG) Study groups (Fractal geometry in geodesy, Regional land and marine geoid modeling, Forward gravity field modeling and global databases, Inverse problems and global optimization, Satellite gravity theory), American Geophysical Union, Canadian Geophysical Union, European Geophysical Union, Chairman of the Graduate studies in Geomatics (UWB), reviewer (Journal of Geodesy, Bollettino di Geofisica Teorica ed Applicata, Studia Geophysica et Geodaetica, Geophysical, Geophysical Journal International, Contributions to Geophysics and Geodesy, Geodetický a kartografický obzor, Czech Science Foundation, IAG Proceedings), Scientific Board of the Faculty of Applied Sciences (UWB)

Research projects

Theoretical and practical refinements of precise geoid determination methods (1996-1999) Canadian government; Transformation of the horizontal datum (1997-1999) Canadian government; Airborne gravimetry for exploration and mapping (1999-2001) Canadian government; Precise geoid determination for georeferencing and oceanography (1999-2001) Canadian government; The GRACE processor for spherical harmonic analysis of temporal variations of geopotential (2002-2004) German government; Experimental research of the Earth's dynamics (2001-2003) Czech government; Determination of precise geoid and quasi-geoid models over the territory of Central Europe (2005-2007) Czech Science Foundation; Progressive collection of spatially-distributed data and their analysis (2006) Czech University Foundation; Design of the knowledge system for decision support based on geodata (2006-2011) Czech government; Continuous and discrete mathematical structures and development of research methods (2005-2011) Czech government; Research Centre of the Earth's Dynamics (2005-2011) Czech government.

Selected peer-reviewed publications (from 45 in total)

– Novák P, Kern M, Schwarz KP (2001) Numerical studies on the harmonic downward continuation of band-limited airborne gravity. *Studia Geophysica et Geodaetica* 45: 327-345

– Novák P, Vaníček P, Martinec Z, Véronneau M (2001) Effects of the spherical terrain on gravity and the geoid. *Journal of Geodesy* 75: 491-504

– Novák P, Heck B (2002) Downward continuation and geoid determination based on band-limited airborne gravity data. *Journal of Geodesy* 76: 269-278

– Novák P, Kern M, Schwarz KP, Sideris MG, Heck B, Ferguson S, Hammada Y, Wei M (2003) On geoid determination from airborne gravity. *Journal of Geodesy* 76: 510-522

– Novák P (2003) Optimal model for geoid determination from airborne gravity. *Studia Geophysica et Geodaetica* 47: 1-36

– Novák P, Bruton AM, Bayoud FA, Kern M, Schwarz KP (2003) On numerical and data requirements for topographical reduction of airborne gravity in geoid determination and resource exploration. *Bollettino di Geodesia e Scienze Affini* 62: 103-124

– Novák P, Kern M, Schwarz KP, Heck B (2003) Evaluation of band-limited topographical effects in airborne gravimetry. *Journal of Geodesy* 76: 597-604

– Novák P (2003) Geoid determination using one-step integration. *Journal of Geodesy* 77: 193-206

– Novák P, Grafarend EW (2005) The ellipsoidal representation of the topographical potential and its vertical gradient. *Journal of Geodesy* 78: 691-706

– Novák P, Grafarend EW (2006) The effect of topographical and atmospheric masses on spaceborne gravimetric and gradiometric data. *Studia Geophysica et Geodaetica* 50: 549-582

– Novák P (2006) Evaluation of local gravity field parameters from high resolution gravity and elevation data. *Contributions to Geophysics and Geodesy 36: 1-33*

55 presentations at conferences worldwide and 60 international citations